Article

Artificial Neural Network Model for the Prediction of Methane Bi-Reforming Products Using CO_2 and Steam

Hao Deng [1,*] **and Yi Guo** [2]

1 School of Electronics and IoT Engineering, Chongqing Industry Polytechnic College, Chongqing 401120, China

2 School of Information Engineering, Chengdu Industry & Trade College, Chengdu 611731, China; guoyi@cdgmxy.edu.cn

* Correspondence: denghao@cqipc.edu.cn

Abstract: The bi-reforming of methane (BRM) is a promising process which converts greenhouse gases to syngas with a flexible H_2/CO ratio. As there are many factors that affect this process, the coupled effects of multi-parameters on the BRM product are investigated based on Gibbs free energy minimization. Establishing a reliable model is the foundation of process optimization. When three input parameters are changed simultaneously, the resulting BRM products are used as the dataset to train three artificial neural network (ANN) models, which aim to establish the BRM prediction model. Finally, the trained ANN models are used to predict the BRM products when the conditions vary in and beyond the training range to test their performances. Results show that increasing temperature is beneficial to the conversion of CH_4. When the molar flow of H_2O is at a low level, the increase in CO_2 can enhance the H_2 generation. While it is more than 0.200 kmol/h, increasing the CO_2 flowrate leads to the increase and then decrease in the H_2 molar flow in the reforming products. When the numbers of hidden layer neurons in ANN models are set as (3, 3), (3, 6) and (6, 6), all the correlation coefficients of training, validation and test are higher than 0.995. When these ANN models are used to predict the BRM products, the variation range of the prediction error becomes narrower, and the standard deviation decreases with the increase in neuron number. This demonstrates that the ANN model with more neurons has a higher accuracy. The ANN model with neuron numbers of (6, 6) can be used to predict the BRM products even when the operating conditions are beyond the training ranges, demonstrating that this model has good extension performance. This work lays the foundation for an artificial intelligent model for the BRM process, and established ANN models can be further used to optimize the operating parameters in future work.

Keywords: methane reforming; syngas production; artificial neural network model; prediction

1. Introduction

Greenhouse gas emission has drawn much attention in recent decades [1–3]. One efficient way to decrease the emission of greenhouse gas is to develop clean energy [4,5]. Under this circumstance, efficient utilization of methane-rich gas, especially natural gas, becomes an important topic [6–8].

Producing syngas, namely H_2 and CO, from methane-rich gas is an industrial means of efficiently utilizing methane-rich gas [7,9]. According to the preparation process, syngas with different compositions can be obtained as feed gas for subsequent ammonia synthesis, Fischer-Tropsch synthesis, methanol production, etc. Processes for preparing syngas from natural gas include steam reforming of methane (SRM), dry reforming of methane (DRM), methane partial oxidation and methane combined reforming, which couples the above processes [10,11]. Methane dry-steam reforming, which is also called bi-reforming of methane (BRM), combines the advantages of both dry reforming and steam reforming [12,13]. In this process, the addition of H_2O can reduce the carbon deposition in the reaction process, and

carbon dioxide is added to adjust the value of the H_2/CO ratio in syngas. This technology can directly utilize biogas, reduce the cost of separation equipment and allow for the flexible adjustment of the H_2/CO ratio for subsequent industrial production. Importantly, both CO_2 and CH_4 are greenhouse gases, which can be efficiently converted to syngas [14]. Therefore, the BRM has been focused on in the field of clean energy.

The methane reforming process involves many side reactions, including the water−gas shift reaction and the formation and digestion of carbon deposition [15]. These reactions have a large impact on catalytic efficiency and sustainability. Therefore, it is very important to consider the optimal reaction conditions from the perspective of thermodynamics to improve the yield of syngas. Thermodynamic analysis plays an important role in the investigation of this technology. It can be used to obtain the optimal operating conditions theoretically and offer a direction for practical operation. Kumar et al. [14] calculated the equilibrium compositions of the BRM process under normal pressure using HSC chemistry. Results demonstrated that steam in BRM could reduce the carbon deposition. Based on the concept of Gibbs free energy minimization, Ozkara [16] analyzed the thermodynamic equilibrium of methane steam and carbon dioxide bi-reforming, which showed that changing the ratio of steam to CO_2 would not affect the consumption rate of CH_4 when the oxidation agent remained constant. Jang et al. [15] conducted an equilibrium analysis on BRM. They investigated the effects of the $(CO_2 + H_2O)/CH_4$ ratio and operating temperature on the conversion of CH_4 and CO_2, the yield of CO, H_2 and C and the ratio of H_2/CO. Thermodynamic evaluation of methane reforming processes with CO_2, $CO_2 + H_2O$, $CO_2 + O_2$ and CO_2+ air was performed in Ref. [17]. Effects of molar feed composition, pressure and temperature were evaluated, which demonstrated that the addition of H_2O or O_2 could reduce the carbon formation. To determine the optimal condition of BRM, effects of temperature, pressure and feed composition of $CH_4/CO_2/H_2O$ on the product distribution were studied based on the thermodynamic equilibrium from Matus et al. [18].
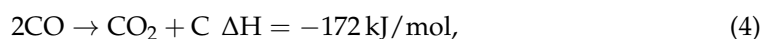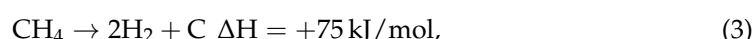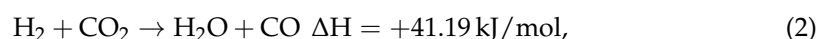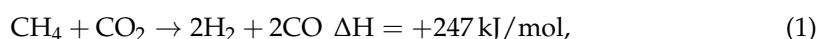
Though these thermodynamic works reveal the basic rules of the methane reforming process, there are many factors that affect the BRM performance simultaneously. Studying the coupled effects of multiple factors is quite necessary for methane reforming as a single variable study always is restricted to the application. Additionally, a useful and reliable model to describe the complex BRM is important for operating parameter optimization. Some works have focused on the coupled effects of operating parameters and the mathematical modelling of BRM. For example, using the Gibbs free energy minimization method, the thermodynamic equilibrium of the BRM process was investigated by Demidov et al. [19]. Coupled effects of CO_2 and H_2O on the products were evaluated. Thermodynamic analysis and optimization combined with response surface methodology for SRM reactions were performed by Özcan et al. [20]. Similarly, Atashi et al. [21] investigated the effects of temperature, pressure, inlet CO_2/CH_4 and their interactions on the DRM. Additionally, a mathematical model was established using response surface methodology. It is observed that the model describing the products of BRM is a strongly non-linear, multi-input and multi-output model. The calculation process based on the Gibbs free energy minimization relates to the state of the thermodynamic system, such as temperature, pressure etc. It should be known that the thermodynamic parameters of all materials are used to calculate the chemical equilibrium. Also, there are some reversible reactions in the BRM process. The chemical equilibrium is changed when there is slight change in the operating condition. If the problem is the calculation of the BRM product, it can be solved. However, when the BRM is used to produce feedstock for the chemical industry, how to determine the operating parameters for the expected product is a problem. If the Gibbs free energy minimization method is used, too many conditions need to be tried to find the proper operating parameters. Thus, the mathematic model is necessary for further parameter optimization. Though response surface methodology can be used to solve this problem, the process is quite complex when the input parameters are high-dimensional. Despite the complex coupling and fitting in response to surface methodology, the equation number to describe the BRM process should be the same as the number of products, which is not

convenient for the utilization of the established model. Additionally, the term number in one equation is related to the number of input parameters. Also, the equation is always an empirical formula. The term number of each equation is also high-dimensional. This causes the mathematical model to be much complex. Artificial intelligence methods have the natural superiority to solve high-dimensional and non-linear problems. It has been widely developed in controlling, modelling, optimizing etc. [22–25]. However, it is a pity that there are few works focusing on the artificial intelligence method for the modelling of the BRM process [26].
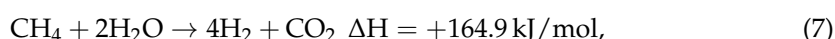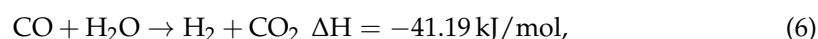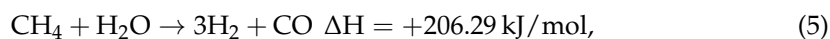
In order to comprehensively investigate the coupled effects of multiple parameters in BRM, a BRM process model is established based on the Gibbs free energy minimization. Operating temperature and feed rates of gases are changed simultaneously to evaluate their coupled effects on the products. Though the products of BRM can be solved based on the Gibbs free energy minimization, it is not a mathematical model while there are complex reactions. If there is a mathematical model which describes this process, the aforementioned problem can easily be solved by using an optimization method. Therefore, the mathematic model establishment of BRM is investigated using artificial neural network (ANN) methodology in this work. It avoids the coupling process of response surface methodology and demonstrates the feasibility of coupling with optimization methods. Additionally, ANN methodology is able to deal with strongly non-linear and high-dimensional problems. In this work, a three-input−five-output ANN is used to model the complex BRM process. Using different neuron numbers in hidden layers, three ANN models are obtained with quite a high accuracy. Finally, these ANN models are used to predict the BRM products when the conditions vary in and beyond the training range to test their performances. This work offers an efficient way to model the BRM process, which can be used in further optimization processes according to the downstream industry.

2. Methane Reforming System and Model

The BRM process is modelled in this work. As it consists of dry reforming and steam reforming, the reaction system is quite complex. In the dry reforming process, greenhouse gases CO_2 and CH_4 are used as feedstock to produce CO and H_2. This process can realize the direct conversion of two kinds of greenhouse gases. This is a way to achieve environmental protection and sustainable development. The main reactions are given as:

$$CH_4 + CO_2 \rightarrow 2H_2 + 2CO \ \Delta H = +247 \, kJ/mol, \tag{1}$$

$$H_2 + CO_2 \rightarrow H_2O + CO \ \Delta H = +41.19 \, kJ/mol, \tag{2}$$

$$CH_4 \rightarrow 2H_2 + C \ \Delta H = +75 \, kJ/mol, \tag{3}$$

$$2CO \rightarrow CO_2 + C \ \Delta H = -172 \, kJ/mol, \tag{4}$$

In the steam reforming process, the main reactions are:

$$CH_4 + H_2O \rightarrow 3H_2 + CO \ \Delta H = +206.29 \, kJ/mol, \tag{5}$$

$$CO + H_2O \rightarrow H_2 + CO_2 \ \Delta H = -41.19 \, kJ/mol, \tag{6}$$

$$CH_4 + 2H_2O \rightarrow 4H_2 + CO_2 \ \Delta H = +164.9 \, kJ/mol, \tag{7}$$

It is seen that reaction (6) is the inverse reaction of (2). In the BRM process, the reforming reactions (1) and (5) are strongly endothermic reactions and need a high temperature to promote the reactions. In dry reforming, due to the existence of the side reaction, inverse water−gas shift, more CO will be produced in the reaction process, and the amount ratio of hydrogen to carbon monoxide in the total reaction product is less than 1. While BRM is conducted, any change in the reactor system can affect the reaction equilibrium.

In this work, the aforementioned reactions take place in a reactor and the reforming products are investigated. In the calculation process, Gibbs free energy minimization with

phase splitting is employed to calculate equilibrium. Simultaneous phase and chemical equilibriums are calculated to obtain the final products of this complex process.

3. Artificial Neural Network Algorithm

In ANN methodology, simulating neuron activity with a mathematical model is an information processing system based on imitating the structure and function of the brain's neural network. In this work, a feedforward and back propagation algorithm is adopted to establish ANN models. For the BRM process, once the flowrate of methane is specified, the other operating parameters are the operating temperature, flowrate of CO_2 and flowrate of steam. From the reactions listed in Section 2, it can be found that the main gaseous products of BRM are H_2, CH_4, H_2O, CO and CO_2. Therefore, in the prediction model of the BRM process, there are three input parameters and five output parameters. The basic structure of the three-input−five-output ANN model is shown in Figure 1.
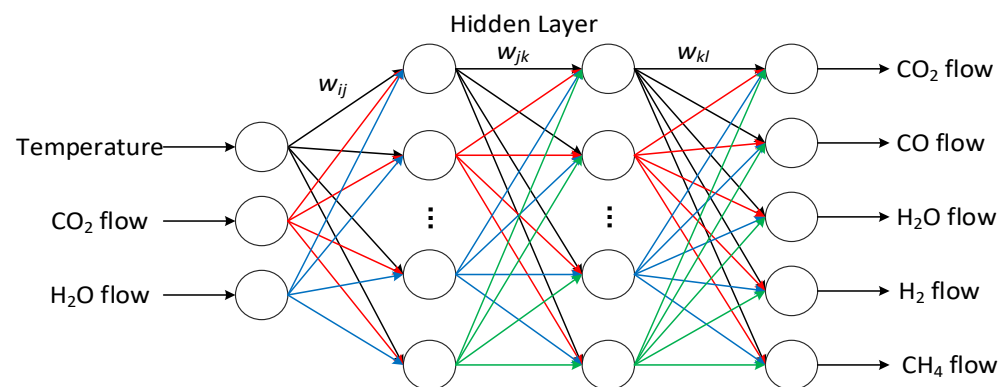
Figure 1. Basic structure of ANN model for product prediction of methane reforming.

Before the prediction, this model should be trained using known information. The main characteristics of the network are signal forward transmission and error back propagation. In the forward transmission, the input signal is processed layer by layer from the input layer through the hidden layer to the output layer. If the output layer cannot be used to obtain the expected output, the back propagation is transferred to adjust the network weight and threshold according to the prediction error.

In this work, the neuron excitation function is chosen as:

$$f(x) = 1 \Big/ (1 + e^{-x})' \tag{8}$$

According to the input vector, the output of the first hidden layer can be calculated as:

$$H_{1j} = f(\sum_{i=1}^{n} w_{ij}x_i - a_{1j}) \; j = 1, 2, \cdots, L, \tag{9}$$

where L is the node number of the first hidden layer; H_j is the output of the first hidden layer; n is the input number, which is 3 in this work; and a is the threshold of the first hidden layer. Using the same concept, the output of the second hidden layer can be calculated, which is denoted as H_{2k}. Then, the output of the output layer can be obtained using the following equation:

$$O_l = \sum_{k=1}^{M} H_{2k}w_{kl} - b_l \; l = 1, 2, \cdots, m, \tag{10}$$

where O is the output; M and m are the numbers of nodes in the second hidden layer and the output parameters, respectively; and b is the threshold of the output layer.

According to the predicted value O and the expected output Y, the prediction error can be obtained as:

$$e_l = Y_l - O_l, \tag{11}$$

The weighting factor w_{kl} can be updated by learning rate η using the following equation:

$$w_{kl} = w_{kl} + \eta H_{2k} e_l, \tag{12}$$

Using same method, the w_{ij} and w_{jk} can also be updated. The threshold of the output layer is updated as:

$$b_l = b_l + e_l, \tag{13}$$

The threshold of the second hidden layer is updated as:

$$a_{2k} = a_{2k} + \eta H_{2k}(1 - H_{2k})\sum_{l=1}^{m} w_{kl}e_l, \tag{14}$$

Correspondingly, the threshold of the first hidden layer is then updated. If the prediction result satisfies the accuracy requirement, the iteration is stopped. The ANN model is well-trained and this model is used for the product prediction of BRM.

4. Methane Reforming Product Results

In this section, the products of the BRM process are investigated. The final products are calculated based on the thermodynamics of the reactants and products. The methane flowrate is set as 1.0 kmol/h. Under the fundamental condition, the reforming temperature is set as 900 °C and the reactions take place at atmospheric pressure. The molar flowrates of CO_2 and H_2O are set as 0.5 kmol/h. When two operating parameters are changed in the following parts, other parameters are kept constant.

4.1. Effects of Flowrates of CO_2 and Steam

In the BRM process, the molar flowrates of steam and CO_2 have coupled effects on the products. Both of them can react with methane, which affects the chemical and phase equilibriums in the reactor. When they are changed from 0 to 1.00 kmol/h, the gaseous products are formed, as shown in Figure 2.
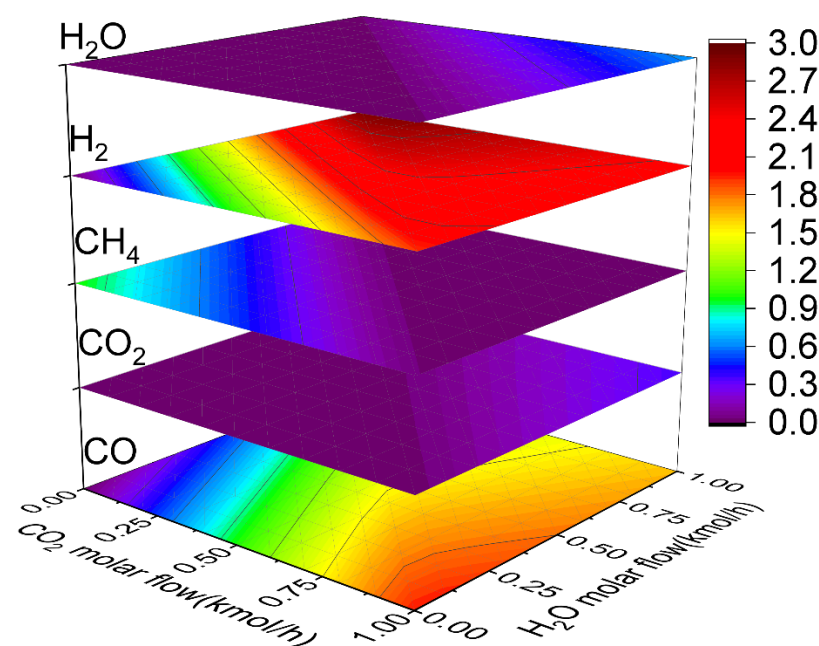

Figure 2. Effects of steam and CO_2 flowrates on gaseous products.

Both the CO_2 and H_2O molar flowrates will affect the concentrations in the reactor. Increasing the CO_2 molar flow is definitely beneficial for the dry reforming of methane, leading to an increase in CO molar flow in the products. When the CO_2 molar flowrate is lower than about 0.400 kmol/h, increasing the steam flow can also promote the conversion of CH_4 and lead to the increase in CO molar flow. When the CO_2 molar flow is further increased, there is competition between the dry reforming and steam reforming processes. The CO flow in the product first increases opposite to the H_2O molar flow into the reactor and then decreases. With the increase in CO_2 molar flow in the reactants, the peak value occurs at a lower value of H_2O flow. In all cases, the maximum molar flow of CO occurs when the molar flowrates of CO_2 and H_2O are 1.000 kmol/h and 0, respectively. The peak value of CO is about 1.952 kmol/h and the H_2 molar flow under this condition is approximately 1.916 kmol/h. As CH_4 is consumed in the BRM process, the molar flow in its products decreases with the increase in CO_2 or H_2O. The minimum value of CH_4 flow in the products is definite in the case that both the CO_2 and H_2O molar flow are 1.000 kmol/h and the minimum value is approximately 0.0009 kmol/h. As the steam and CO_2 cannot be totally converted due to the reversible reactions in the reforming process, the CO_2 and steam flowing in the product increases slightly at the equilibrium state. When the H_2O molar flow increases, the H_2 in the products also rises at a specific flow of CO_2. When the molar flow of H_2O is at a low level, the increase in CO_2 can enhance the H_2 generation. While it is more than 0.200 kmol/h, increasing CO_2 leads to the increase and then decrease in H_2 molar flow in the reforming products. That is due to the fact that high H_2O molar flow can enhance the steam reforming and produce more H_2. The peak value of H_2 molar flow occurs when H_2O and CO_2 molar flows are 1.000 kmol/h and 0, respectively. Under this condition, the H_2 and CO molar flows in products are about 2.900 kmol/h and 0.957 kmol/h, respectively.

4.2. Effects of Flowrate of CO_2 and Temperature

Reaction temperature is an important factor which determines the movement of equilibrium in the BRM process. Therefore, the coupled effects of CO_2 molar flow and temperature are investigated in this part when the temperature varies from 700 °C to 1000 °C. Results are shown in Figure 3.
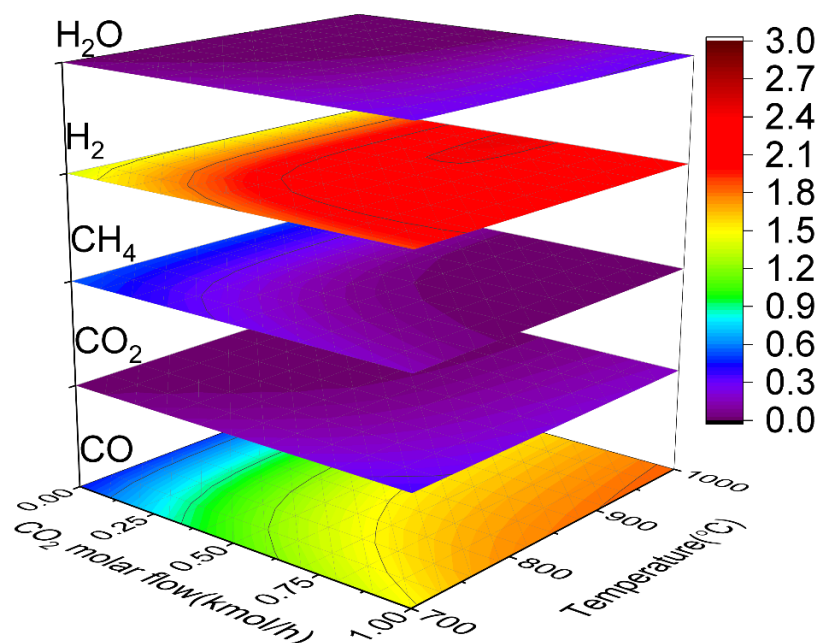
Figure 3. Effects of CO_2 flowrate and temperature on gaseous products.

In this case, the steam molar flow is fixed at 0.5 kmol/h while the CO_2 flow and temperature are changed. Initially, when there is no CO_2 being introduced into the reactor,

this is the SRM process. The SRM process is enhanced with the rise in temperature. When the temperature increases from 700 °C to 1000 °C, the CO and H_2 molar flow increases from 0.441 kmol/h and 1.383 kmol/h to 0.500 kmol/h and 1.500 kmol/h, respectively. The unconverted CH_4 decreases from 0.544 kmol/h to 0.500 kmol/h. The main reactions of methane reforming R1 and R5 are strongly endothermic reactions. Therefore, increasing the temperature is beneficial to both the dry and steam reforming processes. It can be seen that the molar flowrates of CO and H_2 increase opposite to the temperature at any molar flow of CO_2 in the reactants. Also, the enhancement action becomes obvious when the CO_2 molar flow increases. The results in Figure 3 also demonstrate that increasing CO_2 in the reactants can improve the generation of CO in the products. This is due to the fact that it is beneficial to the dry reforming of methane and more CO can be produced. When the CO_2 molar flow and the temperature are 1.000 kmol/h and 1000 °C, respectively, the CO molar flow in the gaseous products reaches a peak value of 1.830 kmol/h. However, its effect on the H_2 generation differs from that of CO. At low temperatures, increasing CO_2 molar flow can enhance the H_2 generation. When the temperature is higher than 770 °C, the H_2 flow in the products increases with the increase in CO_2 molar flow, after which it decreases. It can be seen that the peak value becomes higher when the temperature rises. Additionally, the peak value occurs at a lower CO_2 molar flow when the temperature becomes higher. This might be due to the fact that more CO_2 can intensify the reaction R2, which consumes H_2 and produces more CO. This reaction is also endothermic and therefore, increasing temperature can make it reach equilibrium at a low CO_2 molar flow. The maximum H_2 molar flow is 2.460 kmol/h and it occurs when the temperature and CO_2 molar flow are 1000 °C and 0.5 kmol/h, respectively.

4.3. Effects of Flowrate of H_2O and Temperature

H_2O is one main reactant in the SRM process. Its molar flow in the BRM process determines the chemical and phase equilibriums. In this part, the flowrate of H_2O and operating temperature are changed simultaneously to investigate their coupled effects on the BRM products. The results are shown in Figure 4.
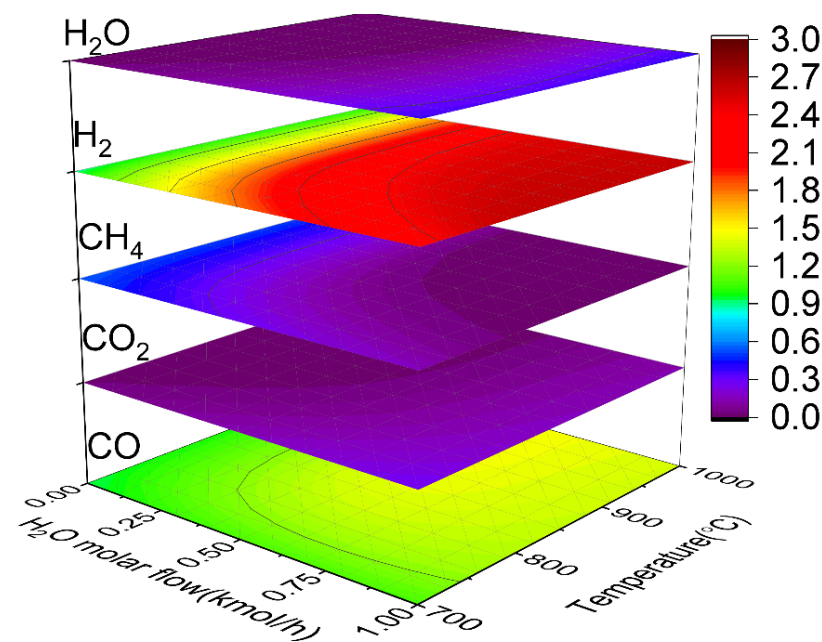
Figure 4. Effects of H_2O flowrate and temperature on gaseous products.

In this process, CH_4 is consumed by CO_2 and H_2O. When the steam molar flow is zero, the results in the figure are the products of DRM with a CO_2 molar flow of 0.500 kmol/h. As increasing temperature and steam flow can promote the conversion of methane, the methane molar flow in products decreases opposite to the temperature and H_2O flow. In

some cases of high H_2O flow and temperature, methane is totally converted. Increasing the H_2O flow into the reaction system definitely enhances the reaction. However, as the chemical equilibrium is related to the gas concentration, the absolute value of the H_2O molar flow becomes higher in the products, though more methane is converted when the H_2O flow into the reaction system increases. As for CO_2, it has a competitive relationship with H_2O. Therefore, increasing inlet H_2O molar flow leads to less consumption of CO_2. Increasing the temperature can enhance the BRM, thus the CO_2 flow decreases with the increase in temperature. The maximum value of CO_2 in the products is approximately 0.281 kmol/h. Due to the fact that increasing temperature and steam flow are beneficial to the methane reforming, the H_2 molar flow in gaseous products directly increases with temperature and H_2O flow. The maximum H_2 molar flow can reach 2.641 kmol/h. Similar to the effect of CO_2 flow on H_2, the CO molar flow also shows the feature of a peak when H_2O flow increases and the temperature is higher. At lower temperatures, increasing H_2O molar flow leads to higher CO molar flow in products monotonically. When the temperature is 1000 °C and H_2O molar flow is 0.5 kmol/h, the maximum CO molar flow occurs, and its value is 1.482 kmol/h.

5. Neural Network Model of the Methane Bi-Reforming System

5.1. Establishment of ANN Model

The previous section exhibited the coupled effects of operating parameters. As mentioned in Section 3, the ANN model is composed of three input parameters. In order to train the ANN model, the compositions of the gaseous products in the BRM process are calculated when temperature, CO_2 flowrate and H_2O flowrate are changed simultaneously. Then, the results are used to train the ANN model.

When temperature, CO_2 flowrate and H_2O flowrate are changed from 700 °C, 0 and 0 to 1000 °C, 1.00 kmol/h and 1.00 kmol/h with intervals of 30 °C, 0.10 kmol/h and 0.10 kmol/h, respectively, 1331 conditions are constructed. Then, the gaseous products are calculated. Before training the ANN model, results under variable conditions and the fundamental condition are ranked randomly. 1300 cases, namely sample datasets, are used to establish the ANN model. Percentages of 70%, 15% and 15% of the samples are used as training datasets, validation datasets and test datasets. The other 32 cases are used in the following process for prediction purposes. In the training process, the number of hidden layers is set as 2. Different numbers of neural nodes are employed. The learning rate is set as 0.05 while the training goal is employed as 10^{-9}. When the number of hidden layer neurons are set as (3, 3), (3, 6) and (6, 6), denoted as 3×3, 3×6 and 6×6, the regression performances of the training process are shown in Figure 5.

During the ANN establishment process, though different numbers of neuron nodes in hidden layers are used, the samples are kept the same in these cases. Therefore, the performances of these established ANN models can be compared. It is seen that the correlation coefficient becomes higher when the node number increases, regardless of what the process is. When the neuron number of hidden layers are chosen as (3, 3), the correlation coefficient in the training process is 0.99605. When the neuron numbers increase to (6, 6) in the hidden layers, the correlation coefficient reaches 0.99996 in the training process. Increasing the neuron numbers is certainly beneficial to improve the accuracy of the ANN model. This can be demonstrated by the correlation coefficient in the test process. As these ANN models have quite a high performance, they are used to predict the BRM products in the following parts.

(**a**)

(**b**)

(**c**)
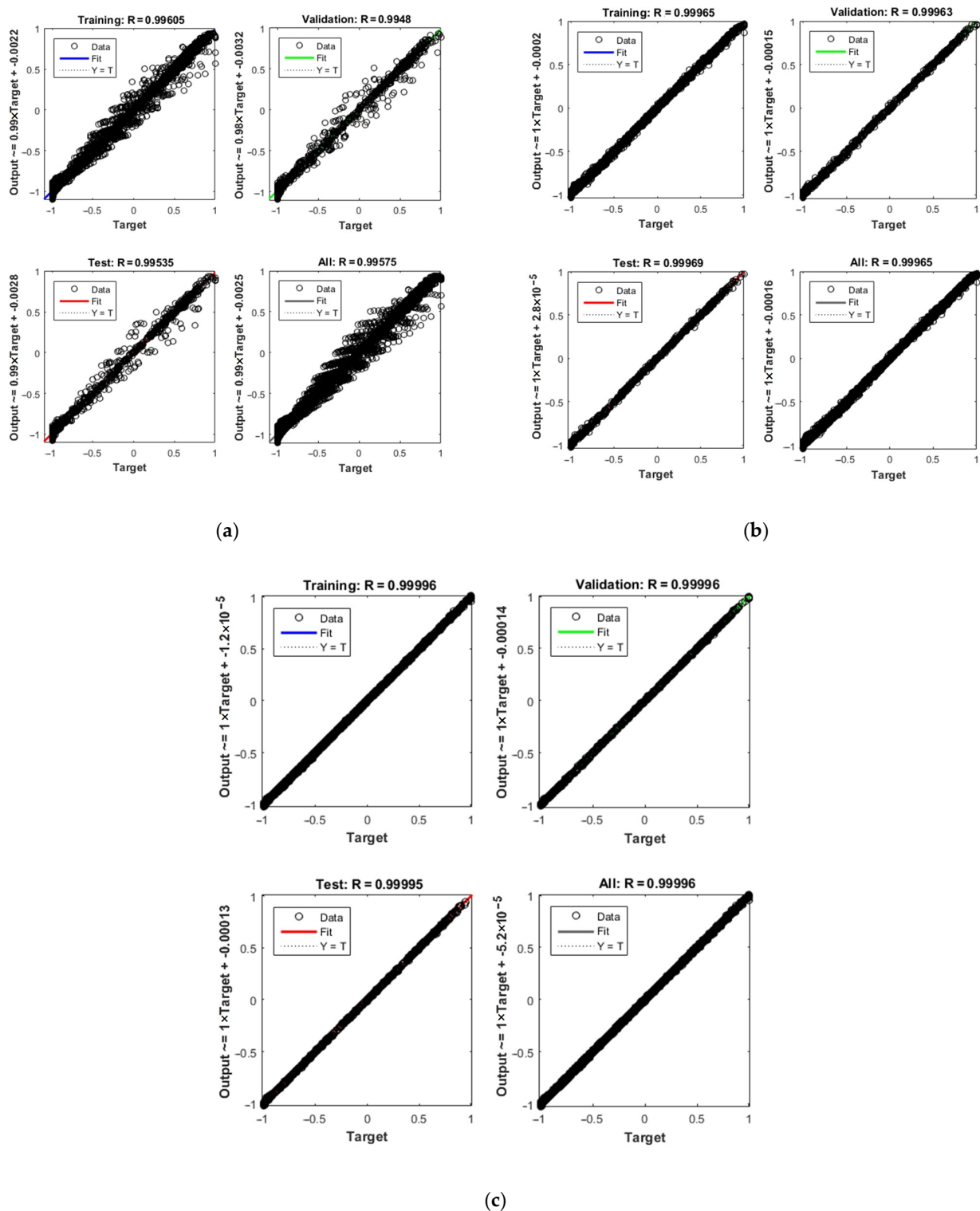
Figure 5. Regression performances of the training process with different numbers of neurons: (**a**) 3 × 3; (**b**) 3 × 6; (**c**) 6 × 6.

5.2. Product Prediction Using Established ANN Models

5.2.1. Prediction of the Cases Varying in the Training Range

As mentioned in the previous part, 32 samples are not used in the ANN model establishment process. Here, the operating parameters in these 32 cases, namely the

temperature, flows of CO_2 and steam, are used as the inputs of the trained and validated ANN models established in Section 5.1. The ANN models are employed to predict the gaseous products of the BRM process. The predicted products are compared with the calculated exact products. The difference between the exact value and predicted value is denoted as the prediction error. The prediction results of the products using different ANN models are given in Figure 6.
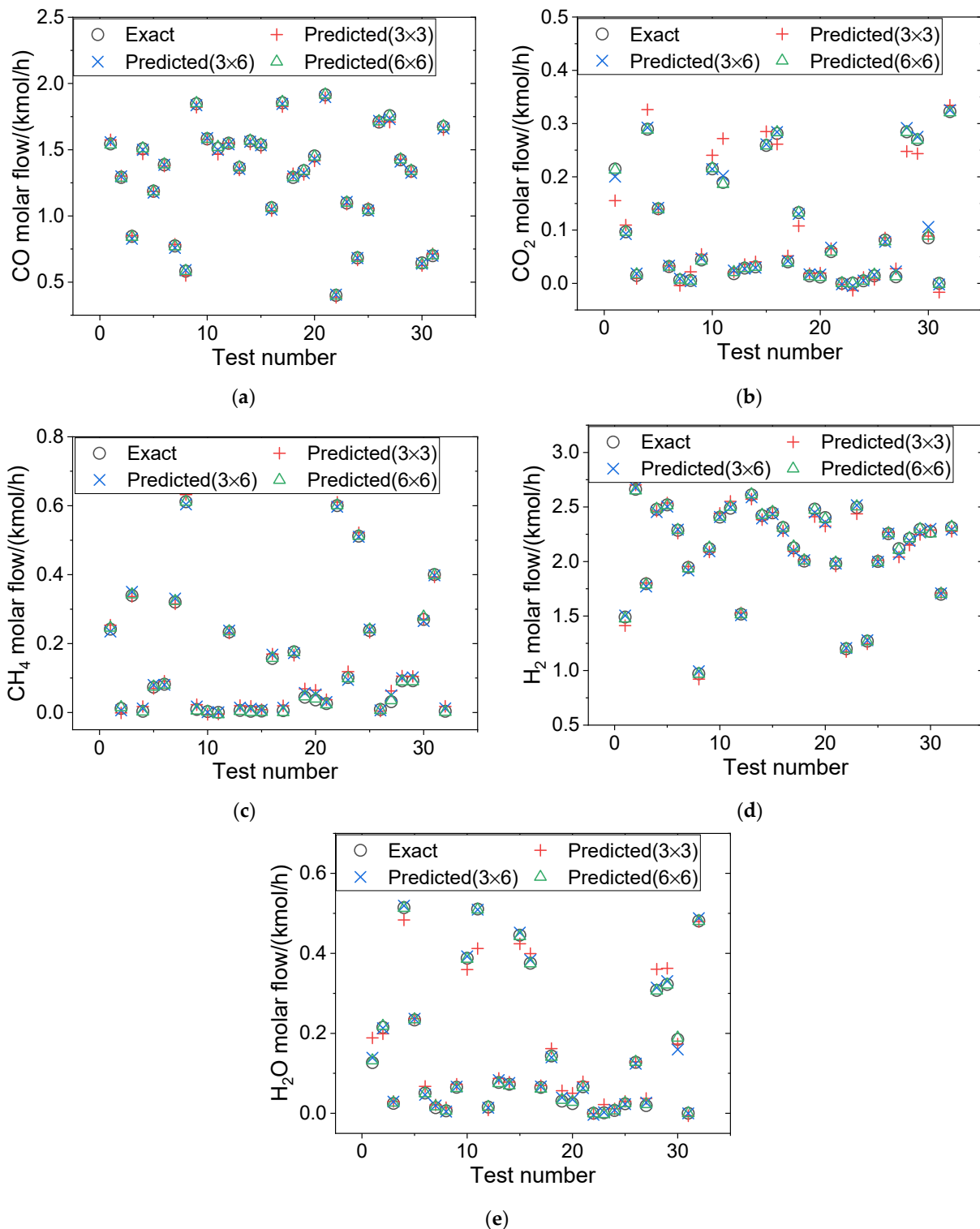
Figure 6. Prediction results of the BRM products using established ANN models: (**a**) CO; (**b**) CO_2; (**c**) CH_4; (**d**) H_2; (**e**) H_2O.

It can be seen that because the operating condition is randomly selected, the results also distribute randomly in these cases. The CO molar flow in the gaseous product varies from 0.400 to 1.915 kmol/h. For the prediction of its value, three ANN models show satisfactory accuracy. The predicted values using these models agree well with the exact values. For CO_2 in the gaseous products, its molar flow varies from 0 to 0.322 kmol/h. As exhibited in Figure 6b, the predicted values in some cases deviate from the exact values with certain errors. It is clear that the deviation range using the ANN model of (3×3) is larger than the deviation range using the model of (6×6), demonstrating the higher accuracy of ANN models with more neurons. This can also be clearly demonstrated by the prediction results of H_2O molar flow in Figure 6e. Additionally, the predicted values of H_2 and CH_4 molar flows can reflect the exact ones, except a few cases using the ANN model with hidden layer neuron numbers of (6×6). Based on these results, the prediction errors are obtained, as illustrated in Figure 7.
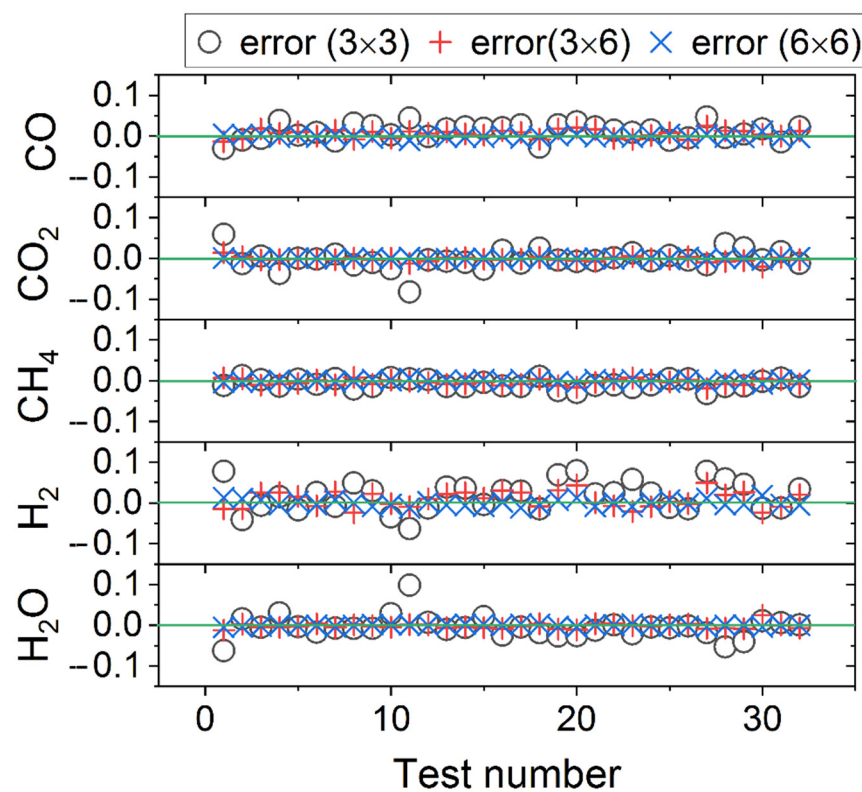
Figure 7. Prediction errors of BRM products.

The prediction errors of these gases using different models are quite low. All of them vary in the range from -0.100 to 0.1000 kmol/h. When the neuron numbers in hidden layers are chosen as (3×3), (3×6) and (6×6), the prediction errors of CO are in the ranges of $[-0.030$ kmol/h, 0.047 kmol/h], $[-0.013$ kmol/h, 0.010 kmol/h] and $[-0.010$ kmol/h, 0.012 kmol/h], respectively. The prediction error ranges of CO_2, CH_4, H_2 and H_2O are $[-0.082$ kmol/h, 0.059 kmol/h], $[-0.031$ kmol/h, 0.013 kmol/h], $[-0.063$ kmol/h, 0.079 kmol/h] and $[-0.062$ kmol/h, 0.098 kmol/h] when the neuron numbers are chosen as (3×3). Also, they are $[-0.004$ kmol/h, 0.003 kmol/h], $[-0.008$ kmol/h, 0.006 kmol/h], $[-0.012$ kmol/h, 0.018 kmol/h] and $[-0.005$ kmol/h, 0.003 kmol/h] when the neuron numbers are (6×6). The error decreases with the increase in neuron number. The standard deviations of the prediction errors are given in Table 1.

Table 1. Standard deviations of the prediction errors using different ANN models.

Neuron Numbers	CO	CO_2	CH_4	H_2	H_2O
(3×3)	0.019	0.024	0.011	0.036	0.027
(3×6)	0.010	0.006	0.007	0.020	0.007
(6×6)	0.004	0.001	0.003	0.008	0.002

It can be seen that with the increase in the neuron number, the variation range becomes narrower and the standard deviation decreases. This demonstrates that the ANN model with more neurons demonstrates higher accuracy.

5.2.2. Prediction of the Cases Varying beyond the Training Range

It can be seen that all ANN models can be used to predict the gaseous products of BRM when the operating conditions vary in the range of the training conditions. To test the imaginable ability of the established ANN models, some random cases are constructed in which no less than one parameter(s) operate(s) beyond the range of training conditions. In these cases, the molar flows of CO_2 or H_2O varies from 0 to 1.5 kmol/h while the temperature is in the range from 600 °C to 1100 °C. The detailed conditions are given in Table 2.

Table 2. Random cases beyond the range of training conditions.

Case Number	1	2	3	4	5	6
CO_2 flow (kmol/h)	1.340	0.324	1.249	0.472	1.117	0.194
H_2O flow (kmol/h)	1.033	1.424	0.725	0.130	0.083	1.239
Temperature (°C)	910	842	603	661	854	899
Case Number	**7**	**8**	**9**	**10**	**11**	**12**
CO_2 flow (kmol/h)	0.759	0.256	0.997	0.075	1.301	0.176
H_2O flow (kmol/h)	1.261	0.048	0.756	1.069	0.812	0.071
Temperature (°C)	707	630	1064	984	821	1028

It can be seen that the variation range in the above table is wider than the range in the training process. At least one operating parameter is beyond the condition range in the training samples. These cases are used to test the potential capability and expansibility of the established ANN models. Using the random conditions as the input parameters of the ANN models, the predicted gaseous products and the calculated products (denoted as exactly one) are illustrated in Figure 8.

From the results in Figure 8, it can be seen that in most cases, the predicted products of BRM can reflect the variation of the exact value. Similar with the previous part, the prediction accuracy is related to the neuron number in the hidden layers, though the range is wider. More neurons can increase the prediction accuracy, making the deviation lower. It is obvious that in these cases, the prediction error in case 3 is the largest and the error increases with the decrease in neuron number. For example, the exact value of CO molar flow is 0.906 kmol/h, while the predicted values are 1.714 kmol/h, 1.234 kmol/h and 1.029 kmol/h when the neuron numbers are (3×3), (3×6) and (6×6), respectively. The predicted products of other gases also show the same trend. This is due to the reason that the condition of case 3 seriously deviates from the condition variation range of the training sample. However, the properly high number of neurons is beneficial to the prediction accuracy. Results in this part demonstrate that the trained ANN models demonstrate sufficient prediction performance, whereas the condition range is wider to some extent.
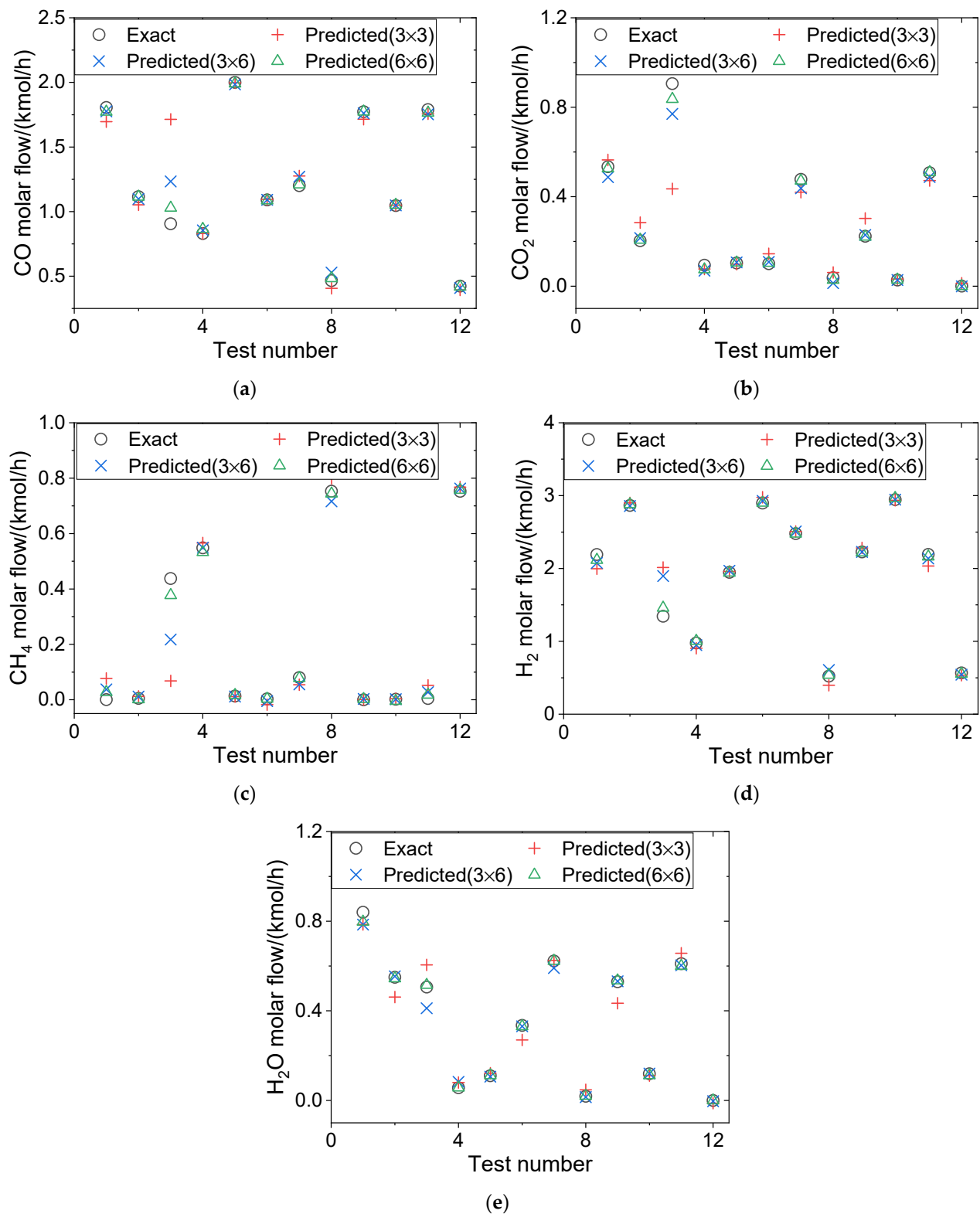
Figure 8. Prediction results of the cases with operating conditions beyond the range of training process: (**a**) CO; (**b**) CO_2; (**c**) CH_4; (**d**) H_2; (**e**) H_2O.

6. Conclusions

As BRM has the advantages of both dry reforming and steam reforming, it has been regarded as one promising technology in the field of clean energy. A BRM model is established based on Gibbs free energy minimization to comprehensively investigate the

coupled effects of multiple parameters. Additionally, ANN models are obtained to predict the products of the complex BRM process with three-input and five-output parameters, which avoids the complex coupling process of response surface methodology. From the results, the following conclusions can be drawn:

(1) When the molar flow of H_2O is at a low level, the increase in CO_2 can enhance the H_2 generation. While it is larger than 0.200 kmol/h, the increase in CO_2 leads to an increase and then a decrease in H_2 molar flow in the reforming products. Increasing temperature can enhance both the steam reforming and dry reforming.

(2) When the neuron numbers of the hidden layers in ANN models are set as (3, 3), (3, 6) and (6, 6), all the correlation coefficients in training, validation and test are higher than 0.995. Also, these ANN models show satisfactory performance for the product prediction when the conditions vary in the training range.

(3) When the condition range varies beyond the training range, the ANN model with 6*6 neuron nodes in the hidden layers has a more favorable performance in the prediction of BRM products.

(4) The established ANN models can be further used to optimize the operating parameters to obtain expected products. In the future, the model can also be improved to predict the BRM products when the conditions vary in a much wider range.

Author Contributions: Data curation, H.D.; methodology, H.D.; software, H.D.; validation, H.D. and Y.G.; formal analysis, Y.G.; investigation, H.D.; writing—original draft preparation, H.D.; writing—review and editing, H.D. and Y.G.; visualization, H.D. and Y.G.; supervision, H.D.; project administration, H.D.; funding acquisition, H.D. All authors have read and agreed to the published version of the manuscript.

Institutional Review Board Statement: Not applicable.

Informed Consent Statement: Not applicable.

Conflicts of Interest: The authors declare no conflict of interest.

References

1. Farooq, S.; Ozturk, I.; Majeed, M.T.; Akram, R. Globalization and CO_2 emissions in the presence of EKC: A global panel data analysis. *Gondwana Res.* **2022**, *106*, 367–378. [CrossRef]
2. Zhang, C.; Xu, T.; Feng, H.; Chen, S. Greenhouse gas emissions from landfills: A review and bibliometric analysis. *Sustainability* **2019**, *11*, 2282. [CrossRef]
3. Eskander, S.M.; Fankhauser, S. Reduction in greenhouse gas emissions from national climate legislation. *Nat. Clim. Chang.* **2020**, *10*, 750–756. [CrossRef]
4. Ghorbani, N.; Aghahosseini, A.; Breyer, C. Assessment of a cost-optimal power system fully based on renewable energy for Iran by 2050–Achieving zero greenhouse gas emissions and overcoming the water crisis. *Renew. Energy* **2020**, *146*, 125–148. [CrossRef]
5. Olabi, A.G.; Abdelkareem, M.A. Renewable energy and climate change. *Renew. Sustain. Energy Rev.* **2022**, *158*, 112111. [CrossRef]
6. Wang, A.; Austin, D.; Song, H. Investigations of thermochemical upgrading of biomass and its model compounds: Opportunities for methane utilization. *Fuel* **2019**, *246*, 443–453. [CrossRef]
7. Knoelchemann, A.; Sales, D.; Silva, M.A.; Abreu, C.A. Performance of Alternative Methane Reforms Based on Experimental Kinetic Evaluation and Simulation in a Fixed Bed Reactor. *Processes* **2021**, *9*, 1479. [CrossRef]
8. Seeburg, D.; Liu, D.; Dragomirova, R.; Atia, H.; Pohl, M.; Amani, H.; Georgi, G.; Kreft, S.; Wohlrab, S. Low-temperature steam reforming of natural gas after LPG-enrichment with MFI membranes. *Processes* **2018**, *6*, 263. [CrossRef]
9. Fatigati, F.; Di Giuliano, A.; Carapellucci, R.; Gallucci, K.; Cipollone, R. Experimental Characterization and Energy Performance Assessment of a Sorption-Enhanced Steam–Methane Reforming System. *Processes* **2021**, *9*, 1440. [CrossRef]
10. Challiwala, M.S.; Ghouri, M.M.; Linke, P.; El-Halwagi, M.M.; Elbashir, N.O. A combined thermo-kinetic analysis of various methane reforming technologies: Comparison with dry reforming. *J. CO2 Util.* **2017**, *17*, 99–111. [CrossRef]
11. Carapellucci, R.; Giordano, L. Steam, dry and autothermal methane reforming for hydrogen production: A thermodynamic equilibrium analysis. *J. Power Sources* **2020**, *469*, 228391. [CrossRef]
12. Moura, I.P.; Reis, A.C.; Bresciani, A.E.; Alves, R. Carbon dioxide abatement by integration of methane bi-reforming process with ammonia and urea synthesis. *Renew. Sustain. Energy Rev.* **2021**, *151*, 111619. [CrossRef]

13. Mohanty, U.S.; Ali, M.; Azhar, M.R.; Al-Yaseri, A.; Keshavarz, A.; Iglauer, S. Current advances in syngas (CO+ H_2) production through bi-reforming of methane using various catalysts: A review. *Int. J. Hydrogen Energy* **2021**, *46*, 32809–32845. [CrossRef]

14. Kumar, N.; Shojaee, M.; Spivey, J.J. Catalytic bi-reforming of methane: From greenhouse gases to syngas. *Curr. Opin. Chem. Eng.* **2015**, *9*, 8–15. [CrossRef]

15. Jang, W.; Jeong, D.; Shim, J.; Kim, H.; Roh, H.; Son, I.H.; Lee, S.J. Combined steam and carbon dioxide reforming of methane and side reactions: Thermodynamic equilibrium analysis and experimental application. *Appl. Energy* **2016**, *173*, 80–91. [CrossRef]

16. Özkara-Aydınoğlu, Ş. Thermodynamic equilibrium analysis of combined carbon dioxide reforming with steam reforming of methane to synthesis gas. *Int. J. Hydrogen Energy* **2010**, *35*, 12821–12828. [CrossRef]

17. Freitas, A.C.; Guirardello, R. Thermodynamic analysis of methane reforming with CO_2, CO_2+ H_2O, CO_2+ O_2 and CO_2+ air for hydrogen and synthesis gas production. *J. CO2 Util.* **2014**, *7*, 30–38. [CrossRef]

18. Matus, E.V.; Sukhova, O.B.; Ismagilov, I.Z.; Kerzhentsev, M.A.; Li, L.; Ismagilov, Z.R. Bi-Reforming of Methane: Thermodynamic Equilibrium Analysis and Selection of Preferable Reaction Conditions. *J. Phys. Conf. Ser.* **2021**, *1749*, 012023. [CrossRef]

19. Demidov, D.V.; Mishin, I.V.; Mikhailov, M.N. Gibbs free energy minimization as a way to optimize the combined steam and carbon dioxide reforming of methane. *Int. J. Hydrogen Energy* **2011**, *36*, 5941–5950. [CrossRef]

20. Özcan, O.; Akın, A.N. Thermodynamic analysis of methanol steam reforming to produce hydrogen for HT-PEMFC: An optimization study. *Int. J. Hydrogen Energy* **2019**, *44*, 14117–14126. [CrossRef]

21. Atashi, H.; Gholizadeh, J.; Tabrizi, F.F.; Tayebi, J.; Mousavi, S.A.H.S. Thermodynamic analysis of carbon dioxide reforming of methane to syngas with statistical methods. *Int. J. Hydrogen Energy* **2017**, *42*, 5464–5471. [CrossRef]

22. Yang, R.; Yan, Y.; Sun, X.; Wang, Q.; Zhang, Y.; Fu, J.; Liu, Z. An Artificial Neural Network Model to Predict Efficiency and Emissions of a Gasoline Engine. *Processes* **2022**, *10*, 204. [CrossRef]

23. Wang, X.; Shao, Y.; Jin, B. Thermodynamic evaluation and modelling of an auto-thermal hybrid system of chemical looping combustion and air separation for power generation coupling with CO_2 cycles. *Energy* **2021**, *236*, 121431. [CrossRef]

24. Yu, X.; Shen, Y.; Guan, Z.; Zhang, D.; Tang, Z.; Li, W. Multi-objective optimization of ANN-based PSA model for hydrogen purification from steam-methane reforming gas. *Int. J. Hydrogen Energy* **2021**, *46*, 11740–11755. [CrossRef]

25. Sener, A.N.; Günay, M.E.; Leba, A.; Yıldırım, R. Statistical review of dry reforming of methane literature using decision tree and artificial neural network analysis. *Catal. Today* **2018**, *299*, 289–302. [CrossRef]

26. Kim, C.H.; Kim, Y.C. Application of artificial neural network over nickel-based catalyst for combined steam-carbon dioxide of methane reforming (CSDRM). *J. Nanosci. Nanotechnol.* **2020**, *20*, 5716–5719. [CrossRef]